TiO2/g-C3N4/SO3H(IL): Unique Usage of Ionic Liquid-Based Sulfonic Acid as an Efficient Photocatalyst for Visible-Light-Driven Preparation of 5-HMF from Cellulose and Glucose

Article *in* ACS Applied Materials & Interfaces · January 2023

DOI: 10.1021/acsami.2c20480

Milad Nayebi
Amirkabir University of Technology

Amir hosein Faraji
Arak University of Technology

Ashkan Bahadoran
Chinese Academy of Sciences

Zhian Jamal Othman
Cihan University

Supporting Information

TiO_2/g-C_3N_4/SO_3H(IL): Unique usage of Ionic Liquid-Based Sulfonic Acid as an Efficient Photocatalyst for Visible-Light-driven Preparation of 5-HMF from Cellulose and Glucose

Milad Nayebi[a], Amir Faraji[b], Ashkan Bahadoran[c], Zhian Jamal Othman[d], Soheila Arghavani[e], Pouya Ghamari Kargar[f]*, Seyed mehrzad Sajjadinezhad[g], and Rajender S. Varma[h]

[a] *Chemical Engineering Department, Amirkabir University of Technology, Tehran, Iran.*

[b] *Assistant Professor, Construction Project Management Dep., Faculty of Architecture, Khatam University, Tehran, Iran; Visiting Fellow, Western Sydney University, Sydney, Australia.*

[c] *State Key Laboratory of Metal Matrix Composite, Shanghai Jiao Tong University, Shanghai 200240, China.*

[d] *Department of physical education and sport sciences, Cihan University-Erbil, Iraq.*

[e, f] *Department of Chemistry, Faculty of Sciences, University of Birjand, Birjand, 97175-615, Iran.*

[g] *Polymer Chemistry Research Laboratory, Faculty of Chemistry, Shahid Beheshti University, Tehran, Iran.*

[h] *Regional Centre of Advanced Technologies and Materials, Czech Advanced Technology and Research Institute, Palacký University in Olomouc, ˇSlechtitelů 27, 783 71, Olomouc, Czech Republic.*

*Corresponding Author: Pouya Ghamari kargar, Email: P.ghamari71@gmail.com

Content:

Materials and Reagents……………………………...…………………………………………………...S2
Figure S1 …………………………...……………………...………………………............................ S3
Figure S2 …………………………...……………………...………………………............................ S4
Figure S3 …………………………...……………………...………………………............................ S5
Figure S4 …………………………...……………………...………………………............................ S6
Table S1. …………………………..……………………………………………………...………........……. S6
Table S2 ……………………………………..…………...……. S7
Table S3 …………………..…………………...……. S7
Figure S5 …………………………...……………………...………………………............................ S8
Figure S6 ………..………………...……………………...………………………............................ S8
References ………………………...……………………...………...……………...…........................... S8

Materials and Reagents

Chemicals, of analytical grade purity, were purchased from Merck Co. (Darmstadt, Germany) and were used as received. FT-IR spectra were secured deploying a Perkin-Elmer 781 spectrophotometers using pressed KBr discs. NP dispersion and morphology and NP dispersion were realized employing scanning electron microscopy (FESEM, Cam scan MV2300). The chemical structural integrity of the obtained nano catalyst was affirmed by energy-dispersive X-ray spectroscopy (EDX). The X-ray diffraction (XRD) spectra were obtained by utilizing a Philips powder diffractometer type PW 1373, equipped with a graphite monochromator crystal. The X-ray wavelength deployed was 1.54 Å and the diffraction patterns were secured in the 2h intervals (10-80) using a scanning rate of 1°/min. Ultrasonic generation was accomplished using an ultrasonic bath, Bandelin electronic at a frequency of 35 KHz. Thermogravimetric analysis (TGA) was performed using STA 1500 Rheometric Scientific (England) for the as-obtained catalyst and was carried out under constant N_2 gas flow from 25 to 1000 °C at a temperature gradient of 10 °C min^{-1}. The size and shape of the TiO_2/g-C_3N_4/SO_3H(IL) nanocomposite were determined using Philips EM208 and JEOL JEM-3010 transmission electron microscope (TEM). Elemental analyses were completed employing a PerkinElmer elemental analyzer for C, H, N, O determination. Inductively coupled plasma atomic emission spectroscopic (ICP-AES) analysis was performed deploying OPTIMA 7300DV equipment.

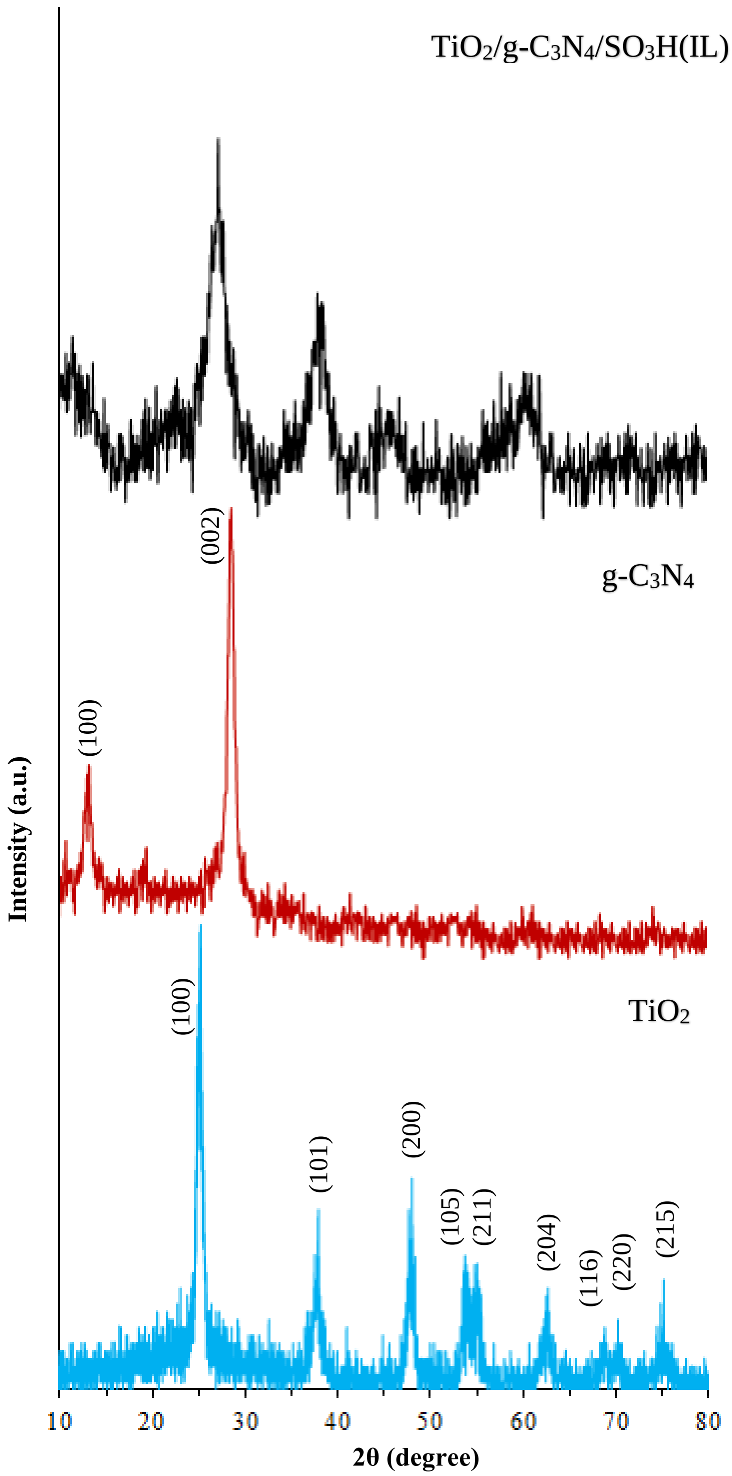

Figure S1: XRD spectra of nanostructure TiO_2, g-C_3N_4, and TiO_2/g-C_3N_4/SO_3H(IL) nanocomposite

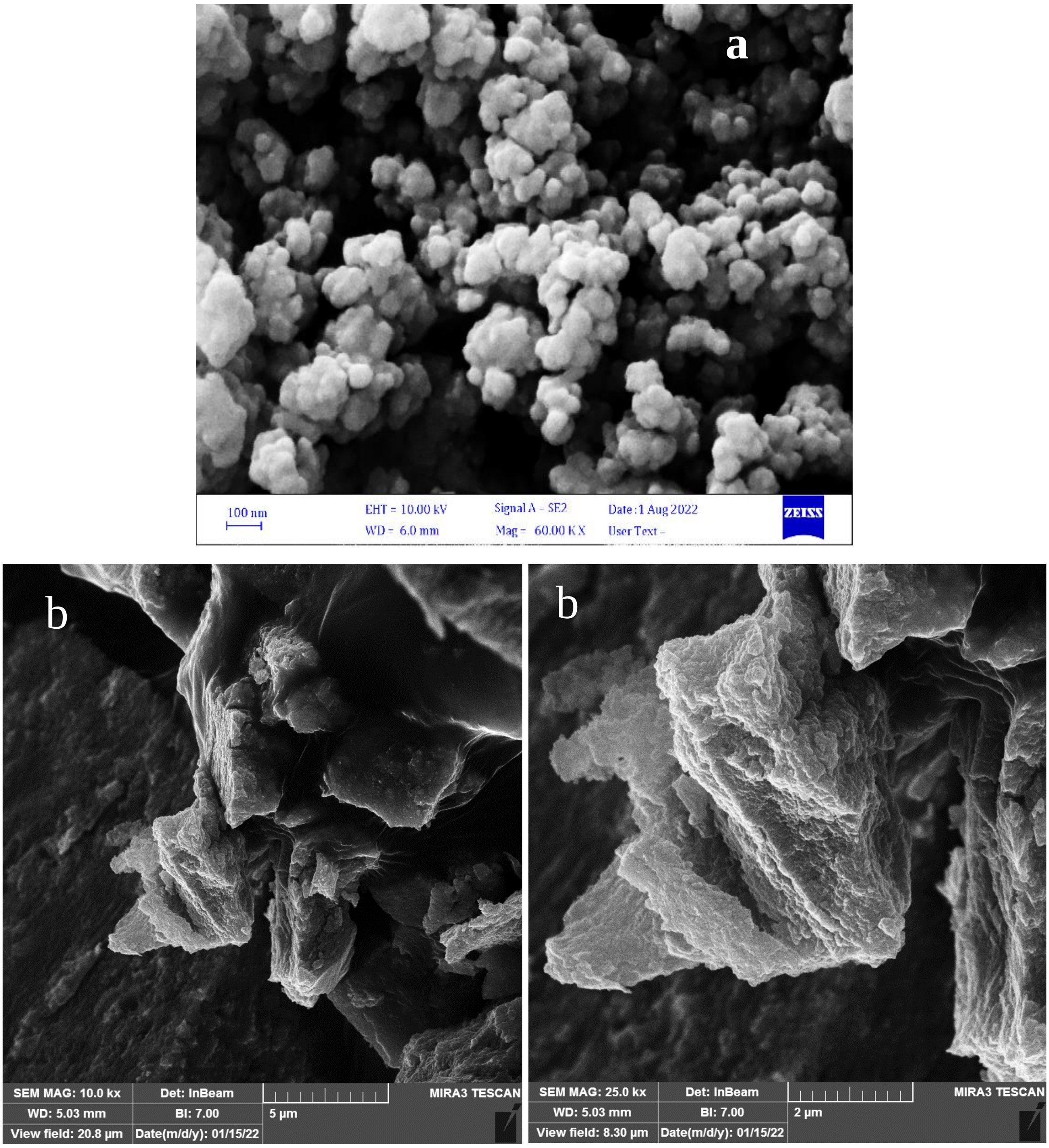

Figure S2: FESEM images (a) TiO_2 and (b) TiO_2/g-C_3N_4/SO_3H(IL)

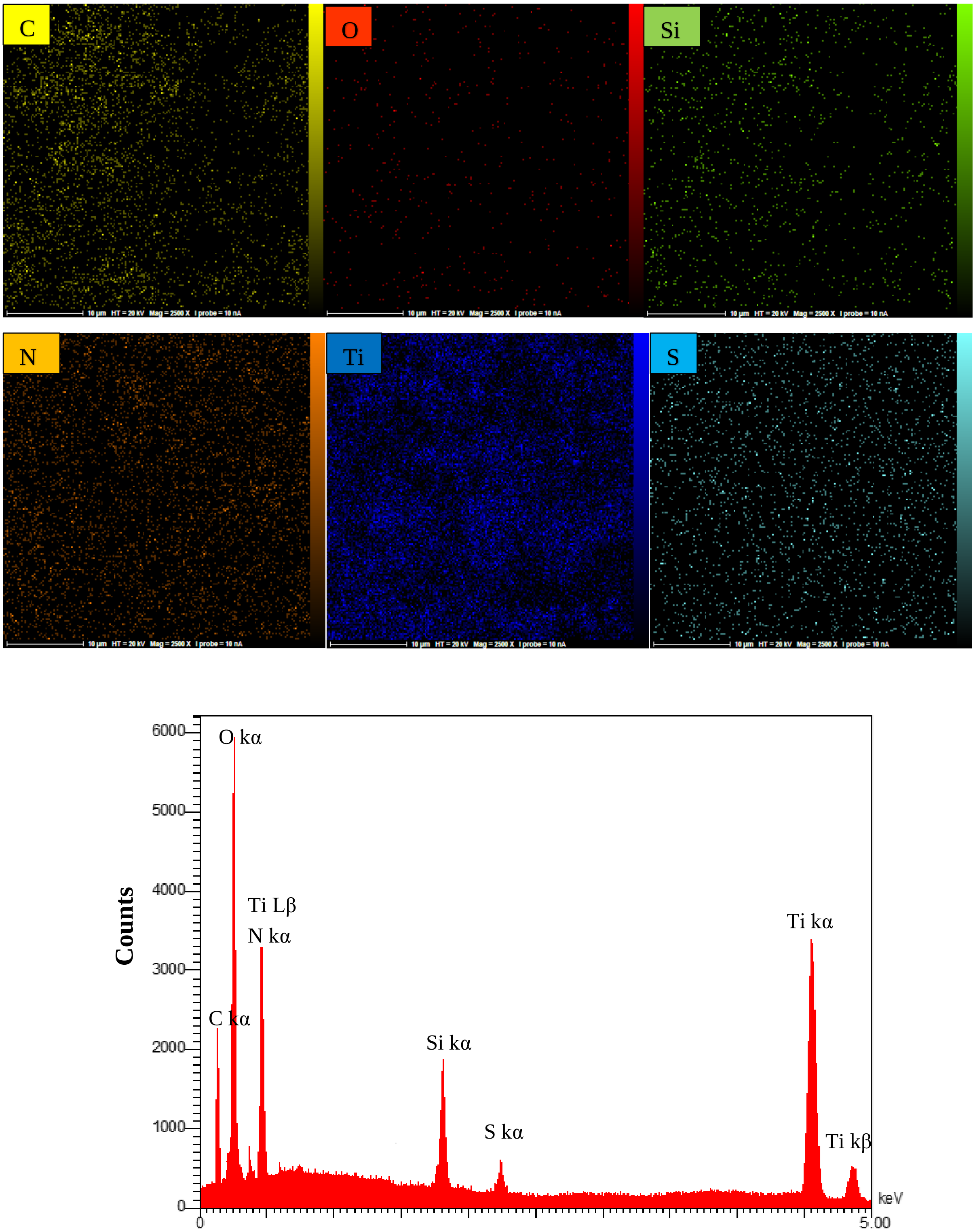

Figure S3: EDX and mapping images for the $TiO_2/g\text{-}C_3N_4/SO_3H$(IL) nanocomposite

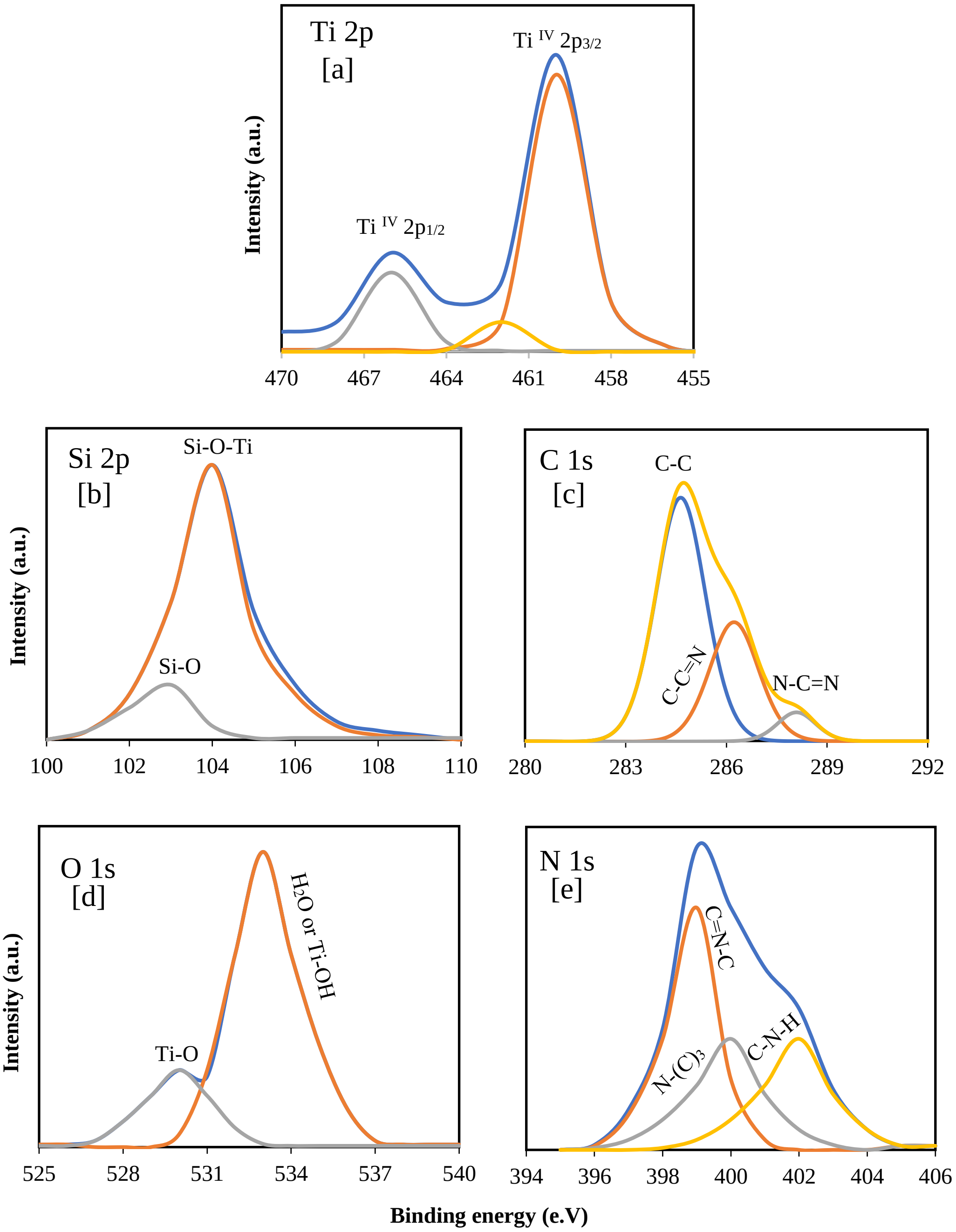

Figure S4: XPS spectra of the TiO_2/g-C_3N_4/SO_3H(IL) nanocomposite: Peak deconvolution of (a) Ti 2p, (b) Si 2p, (c) C 1s, (d) O 1s, and (e) N 1s.

Table S1: Comparison of the Band Gap (Eg), VB, and CB of g-C_3N_4, TiO_2, and TiO_2/g-C_3N_4/SO_3H(IL) nanocomposite samples

Sample	E_g/eV	VB	CB
g-C_3N_4	2.70	1.40	-1.3
TiO_2 Anatase	3.2	2.7	-0.5
TiO_2/g-C_3N_4/SO_3H(IL)	2.47	1.97	-0.54

Table S2: Textual characteristics of g-C_3N_4, TiO_2, and TiO_2/g-C_3N_4/SO_3H(IL) nanocomposite samples.

Sample	Surface area (m^2. g^{-1})	Pore volume (cm^3. g^{-1})	Average pore diameter (nm)
g-C_3N_4	33.75	0.1	123
Anatase TiO_2	177.23	0.9	5.5
TiO_2/g-C_3N_4/SO_3H(IL)	181.75	1.97	6.2

Table S3: Comparison of the catalytic performance of TiO_2/g-C_3N_4/SO_3H(IL) with other documented solid acid catalysts etc. for 5-HMF Production

Substrate	Catalyst	Condition	Time (h)	5-HMF yield (%)	Ref.
Glucose	TiO_2/g-C_3N_4/SO_3H(IL)	H_2O, Blue LED, 100 ºC	1	96	**This work**
Glucose	LSP	S.F., 135 ºC	0.5	9	1
Glucose	nano-POM/nano-ZrO_2/nano-γ -Al_2O_3	Acetone/DMSO, 190 ºC	4	60.1	2
Glucose	H_2SO_4	GVL, 130 ºC	1	13	3
Glucose	$Nb_{0.2}$-WO_3	H_2O, 120 ºC	6	36	4
Glucose	B-SO_3H	H_2O, 150 ºC	4	39	5
Glucose	m-ZrP-600	H_2O, 155 ºC	6	46	6
Glucose	SPPS	[EMIM]Br, 140 ºC	4	87	7
Glucose	S-GCN	H_2O, 200 ºC	5	93	8
Glucose	Al-KCC-1	DMSO, 170 ºC	2	93	9
Cellulose	TiO_2/g-C_3N_4/SO_3H(IL)	H_2O, Blue LED, 100 ºC	1.5	92	**This work**
Cellulose	NaCl	THF/H_2O, 200 ºC	6-8	56-59	10
Cellulose	$ChH_2PW_{12}O_{40}$	MIBK/H_2O, 140 ºC	8	75	11
Cellulose	Nb–C-50	THF/H_2O, NaCl, 170 ºC	8	53	12
Cellulose	Nin/Cs	H_2O, 200 ºC	1	85	13
Cellulose	$HfO(PO_4)_{2.0}$	THF/H_2O, NaCl, 190 ºC	4	89.7	14
Cellulose	Cr-ACS	BmimCl/H_2O, 120 ºC	1	49	15
Cellulose	P-TiO_2	H_2SO_4-Ballmilled, NMP THF/H_2O, 180 ºC	1.6	86	16
Cellulose	Bimodal-HZ-5	H_2O, 190 ºC	4	46	17
Cellulose	$AlCl_3$•$6H_2O$	THF/H_2O, Microwave, 180 ºC	0.5	37	18

NMP: N-Methyl-2-pyrrolidone

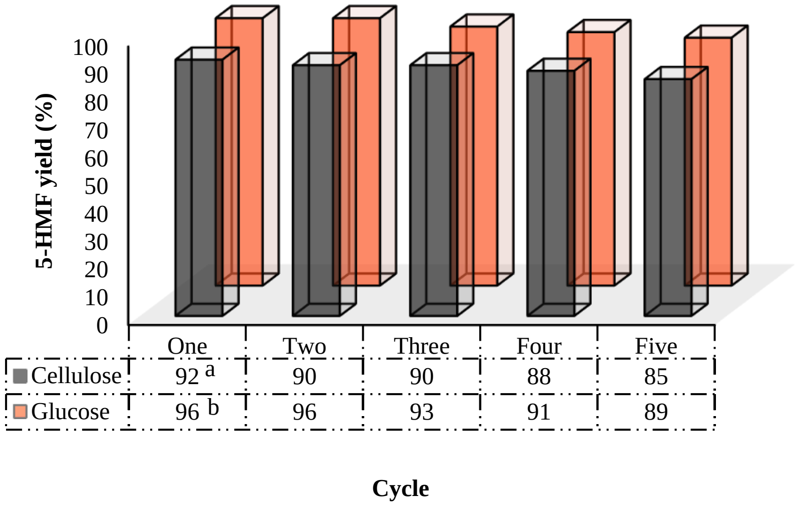

Figure S5: Reusability test of photocatalyst for glucose and cellulose dehydration. [a, b] Isolated yield

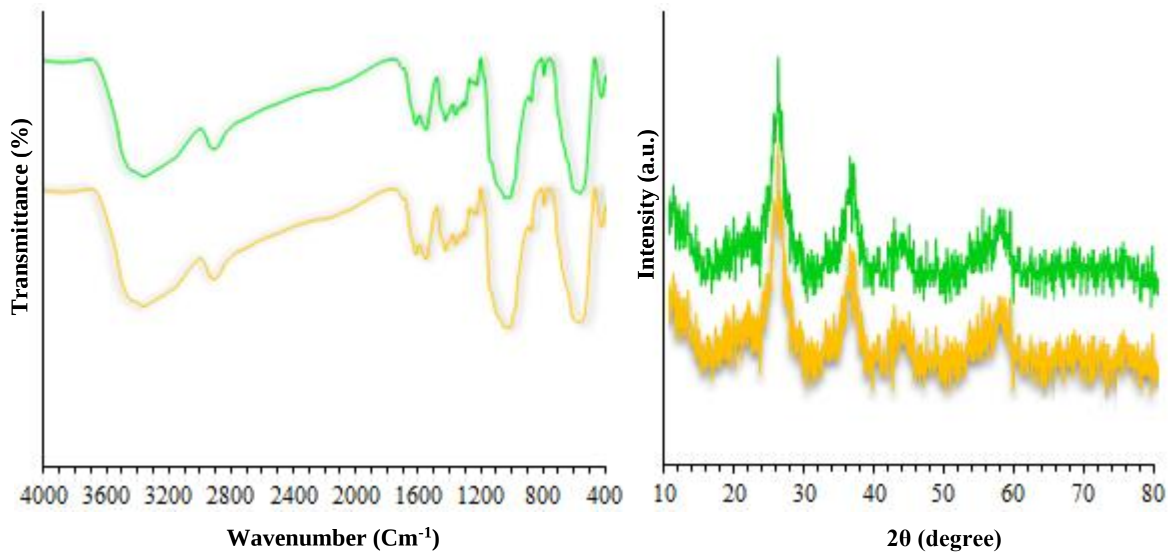

Figure S6: The FT-IR, and XRD analysis of the recovered TiO_2/g-C_3N_4/SO_3H(IL) photocatalyst after the 5 runs (Green: Cellulose, and Yellow: Glucose).

References

(1) Bhaumik, P.; Chou, H.-J.; Lee, L.-C.; Chung, P.-W. Chemical Transformation for 5-Hydroxymethylfurfural Production from Saccharides Using Molten Salt System. *ACS Sustain. Chem. Eng.* **2018**, *6* (5), 5712–5717. https://doi.org/10.1021/acssuschemeng.7b04815.

(2) Teimouri, A.; Mazaheri, M.; Chermahini, A. N.; Salavati, H.; Momenbeik, F.; Fazel-Najafabadi, M. Catalytic Conversion of Glucose to 5-Hydroxymethylfurfural (HMF)

Using Nano-POM/Nano-ZrO2/Nano-γ-Al2O3. *J. Taiwan Inst. Chem. Eng.* **2015**, *49*, 40–50. https://doi.org/10.1016/j.jtice.2014.11.015.

(3) Qi, L.; Mui, Y. F.; Lo, S. W.; Lui, M. Y.; Akien, G. R.; Horváth, I. T. Catalytic Conversion of Fructose, Glucose, and Sucrose to 5-(Hydroxymethyl)Furfural and Levulinic and Formic Acids in γ-Valerolactone As a Green Solvent. *ACS Catal.* **2014**, *4* (5), 1470–1477. https://doi.org/10.1021/cs401160y.

(4) Yue, C.; Li, G.; Pidko, E. A.; Wiesfeld, J. J.; Rigutto, M.; Hensen, E. J. M. Dehydration of Glucose to 5-Hydroxymethylfurfural Using Nb-Doped Tungstite. *ChemSusChem* **2016**, *9* (17), 2421–2429. https://doi.org/10.1002/cssc.201600649.

(5) Howard, J.; Rackemann, D. W.; Bartley, J. P.; Samori, C.; Doherty, W. O. S. Conversion of Sugar Cane Molasses to 5-Hydroxymethylfurfural Using Molasses and Bagasse-Derived Catalysts. *ACS Sustain. Chem. Eng.* **2018**, *6* (4), 4531–4538. https://doi.org/10.1021/acssuschemeng.7b02746.

(6) Saravanan, K.; Park, K. S.; Jeon, S.; Bae, J. W. Aqueous Phase Synthesis of 5-Hydroxymethylfurfural from Glucose over Large Pore Mesoporous Zirconium Phosphates: Effect of Calcination Temperature. *ACS Omega* **2018**, *3* (1), 808–820. https://doi.org/10.1021/acsomega.7b01357.

(7) Li, Z.; Su, K.; Ren, J.; Yang, D.; Cheng, B.; Kim, C. K.; Yao, X. Direct Catalytic Conversion of Glucose and Cellulose. *Green Chem.* **2018**, *20* (4), 863–872. https://doi.org/10.1039/C7GC03318D.

(8) Chhabra, T.; Bahuguna, A.; Dhankhar, S. S.; Nagaraja, C. M.; Krishnan, V. Sulfonated Graphitic Carbon Nitride as a Highly Selective and Efficient Heterogeneous Catalyst for the Conversion of Biomass-Derived Saccharides to 5-Hydroxymethylfurfural in Green Solvents. *Green Chem.* **2019**, *21* (21), 6012–6026. https://doi.org/10.1039/C9GC02120E.

(9) Shahangi, F.; Najafi Chermahini, A.; Saraji, M. Dehydration of Fructose and Glucose to 5-Hydroxymethylfurfural over Al-KCC-1 Silica. *J. Energy Chem.* **2018**, *27* (3), 769–780. https://doi.org/10.1016/j.jechem.2017.06.004.

(10) Li, X.; Zhang, Y.; Xia, Q.; Liu, X.; Peng, K.; Yang, S.; Wang, Y. Acid-Free Conversion of Cellulose to 5-(Hydroxymethyl)Furfural Catalyzed by Hot Seawater. *Ind. Eng. Chem. Res.* **2018**, *57* (10), 3545–3553. https://doi.org/10.1021/acs.iecr.8b00443.

(11) Zhang, X.; Zhang, D.; Sun, Z.; Xue, L.; Wang, X.; Jiang, Z. Highly Efficient Preparation of HMF from Cellulose Using Temperature-Responsive Heteropolyacid Catalysts in Cascade Reaction. *Appl. Catal. B Environ.* **2016**, *196*, 50–56. https://doi.org/10.1016/j.apcatb.2016.05.019.

(12) Li, X.; Peng, K.; Xia, Q.; Liu, X.; Wang, Y. Efficient Conversion of Cellulose into 5-Hydroxymethylfurfural over Niobia/Carbon Composites. *Chem. Eng. J.* **2018**, *332*, 528–536. https://doi.org/10.1016/j.cej.2017.06.105.

(13) Wu, Q.; Zhang, G.; Gao, M.; Cao, S.; Li, L.; Liu, S.; Xie, C.; Huang, L.; Yu, S.; Ragauskas, A. J. Clean Production of 5-Hydroxymethylfurfural from Cellulose Using a Hydrothermal/Biomass-Based Carbon Catalyst. *J. Clean. Prod.* **2019**, *213*, 1096–1102. https://doi.org/10.1016/j.jclepro.2018.12.276.

(14) Liu, H.; Cao, X.; Wei, J.; Jia, W.; Li, M.; Tang, X.; Zeng, X.; Sun, Y.; Lei, T.; Liu, S.;

Lin, L. Efficient Aerobic Oxidation of 5-Hydroxymethylfurfural to 2,5-Diformylfuran over Fe_2O_3 -Promoted MnO 2 Catalyst. *ACS Sustain. Chem. Eng.* **2019**, *7* (8), 7812–7822. https://doi.org/10.1021/acssuschemeng.9b00010.

(15) Tyagi, U.; Anand, N.; Kumar, D. Synergistic Effect of Modified Activated Carbon and Ionic Liquid in the Conversion of Microcrystalline Cellulose to 5-Hydroxymethyl Furfural. *Bioresour. Technol.* **2018**, *267*, 326–332. https://doi.org/10.1016/j.biortech.2018.07.035.

(16) Atanda, L.; Shrotri, A.; Mukundan, S.; Ma, Q.; Konarova, M.; Beltramini, J. Direct Production of 5-Hydroxymethylfurfural via Catalytic Conversion of Simple and Complex Sugars over Phosphated TiO 2. *ChemSusChem* **2015**, *8* (17), 2907–2916. https://doi.org/10.1002/cssc.201500395.

(17) Nandiwale, K. Y.; Galande, N. D.; Thakur, P.; Sawant, S. D.; Zambre, V. P.; Bokade, V. V. One-Pot Synthesis of 5-Hydroxymethylfurfural by Cellulose Hydrolysis over Highly Active Bimodal Micro/Mesoporous H-ZSM-5 Catalyst. *ACS Sustain. Chem. Eng.* **2014**, *2* (7), 1928–1932. https://doi.org/10.1021/sc500270z.

(18) Yang, Y.; Hu, C.; Abu-Omar, M. M. Conversion of Carbohydrates and Lignocellulosic Biomass into 5-Hydroxymethylfurfural Using $AlCl_3{\cdot}6H_2O$ Catalyst in a Biphasic Solvent System. *Green Chem.* **2012**, *14* (2), 509–513. https://doi.org/10.1039/C1GC15972K.